London '13

We 11 06

Full Waveform Inversion in a Complex Geological Setting - A Narrow Azimuth Towed Streamer Case Study from the Barents Sea

C.E. Jones* (BG Group), M. Evans (CGG), A. Ratcliffe (CGG), G. Conroy (CGG), R. Jupp (CGG), J.I. Selvage (BG Group) & L. Ramsey (BG Norge)

SUMMARY

We apply Full Waveform Inversion (FWI) to a Narrow Azimuth (NAZ) towed streamer data acquired over the Samson Dome region in the Barents Sea which has complex structural geology. This case study demonstrates the improvement in seismic image quality resulting from dramatically increasing the wavenumber content in the velocity field using FWI. The FWI result shows a spatial consistency that was unexpected from a standard 3D NAZ dataset. It also demonstrates the potential use of FWI velocity models in geological interpretation and shallow geohazard detection, even though in this implementation the FWI is effectively solving a combination of velocity, anisotropy and density, rather than just P-wave velocity.

Introduction

In recent years, the application of Full Waveform Inversion (FWI) to real world sized 3D datasets using acoustic approximations of seismic waves has become a reality, driven primarily by a significant increase in computing power. The literature contains many real data examples demonstrating the generation of high-resolution velocity models from FWI. Many of these case studies use ideal acquisition geometries with large offset and azimuth ranges, often from ocean bottom cable/node (OBC/OBN) surveys.

In this paper, we present a case study of applying FWI to a 3D Narrow Azimuth (NAZ) towed streamer dataset from the Barents Sea, comprising a total survey acquisition area of 1790 km^2, and successfully demonstrate a spatially consistent velocity field from the FWI leading to improved reflection imaging. We also evaluate different starting velocity models, but we did not perform a travel-time reflection tomography to establish a starting model since the pre-stack reflection data was too poor to obtain reliable pre-stack picks from common image gathers. In addition, as shown below, our ultimate choice of starting model proved adequate and a travel-time reflection tomography project was expected to take a similar time to the four month lifespan of the FWI project.

Barents Sea case study area

The area of interest is over the Samson Dome, located in the Barents Sea, Norway (licence PL 534). The top of the dome has been removed by a significant erosional unconformity and overlain by Quaternary sediments, including areas of high amplitude potentially associated with shallow gas. This complex geology in the shallow section, in combination with radial faulting at the crest of the dome below the unconformity, has the potential for large, rapid velocity variations.

This complex velocity field has previously led to poor signal-to-noise in the Pre-Stack Time Migration (PreSTM) gathers under the crest of the dome. Since reflection tomography relies on picking events on these gathers, this area was considered to be very challenging to make reflection travel-time tomography provide a stable solution to the shallow velocity model. Thus, FWI was selected in an attempt to define the complex, shallow velocity model before re-migrating the data.

FWI test details

The FWI algorithm is a 3D time-domain approach that is currently driven by the transmitted arrivals (diving and head waves). We use the standard low→high frequency strategy to reduce the likelihood of the FWI velocity model falling into a local minimum. That said, one of the prerequisites for FWI to work is to have events on the real and modelled shot records that are not cycle skipped. This cycle skipping criteria is controlled by the combination of the starting velocity model and the lowest usable frequency in the real data. As a consequence, careful denoising of low frequency data to improve the signal-to-noise is required. For this study the raw shot data had swell noise attenuation and linear radon de-noise processes applied. The only additional pre-processing on the real data is a band-pass filter, 2-7 Hz, and an inner and outer mute to highlight the transmitted energy. A selection of methods were used to generate possible starting velocity models for the FWI: (1) a constrained Dix inversion of the PreSTM RMS velocity field stretched to depth, (2) a well-based blocky velocity model and (3) velocities from first arrival refraction tomography. In this case, we found that (1) the PreSTM derived velocity field when combined with a blocky anisotropy model produced modelled shots that were not cycle skipped at the lowest available frequency in the real data (Figure 1) and this was used as the starting model. To generate the synthetic shot records used in the FWI process, a modelled source wavelet, filtered to match the seismic data, but with no source or receiver ghosts, was used in combination with a free-surface in the wave equation modelling. More details on the FWI algorithm, methodology and workflow are given in Warner et al. (2010) and Ratcliffe et al. (2011).

The acquisition was NAZ marine with 10 streamers, each 6 km long, with 100 m between the cables and a 12.5 m flip-flop shot interval, covering a full fold FWI update area of 1060 km^2. Given the

maximum offset in the data of 6.2 km, ray-based modelling of the diving waves through the starting model indicated an expected maximum depth of penetration of ~1.5 km below the sea-surface. With regard to the lowest frequency available in the data: there was no low-cut in the recording system and the nominal shot and receiver depths were 5 and 7 m, respectively. These acquisition parameters, together with the aforementioned processing, gave rise to a lowest useable frequency of 4Hz. Consequently, the FWI was run in cascaded passes of 4 different frequency bands, starting at [2, 4] Hz and going up to [2, 7] Hz, incrementing 1 Hz in bandwidth at each frequency band.

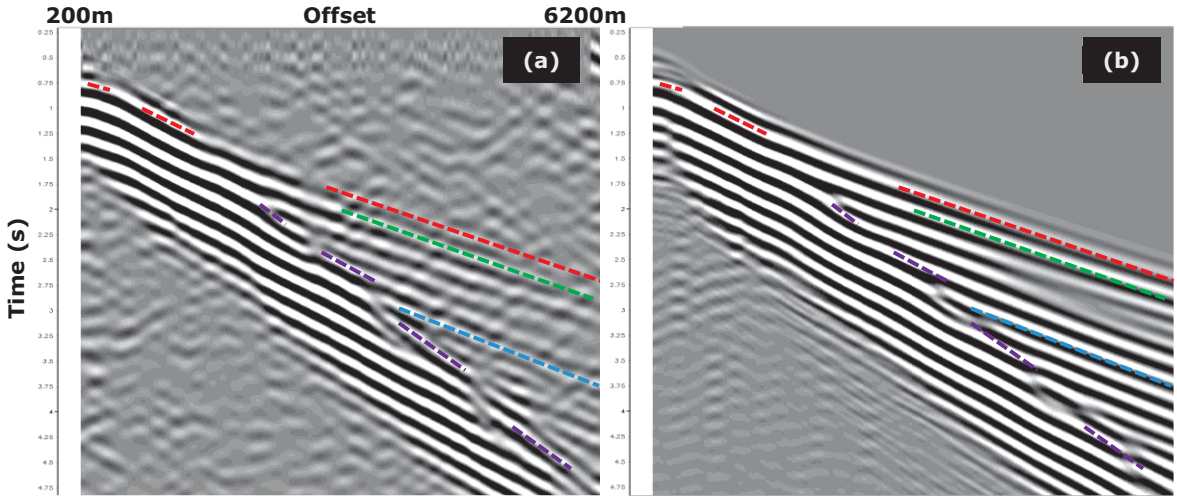

Figure 1: (a) Filtered field data, and (b) forward modelled shot using starting velocity model. The coloured dashed lines offer reference points on both figures to aid timing comparison.

FWI results

Figure 2 shows depth slices through the starting velocity model at 1100 and 1350 m, this is ~850 and 1100 m below the water bottom, respectively. The corresponding depth slices of the FWI derived model are shown in Figure 3. The improvement in resolution and geological conformability of the FWI velocity model is quite dramatic, especially as this is from a non-overlapping NAZ survey. Figure 4 shows the same display with a seismic depth slice overlaid – there is a striking agreement between the velocities and the seismic image. Note that the FWI velocity field contained a significant sail-line orientated acquisition footprint, which was subsequently attenuated by a spatial filter applied across the sail-lines (Figure 5). The improvement in imaging from the FWI velocity model is demonstrated by flatter Kirchhoff common image gathers in Figure 6 and increased stack response and continuity on the Kirchhoff pre-stack depth migrations in Figure 7.

Discussion

It is clear that the application of FWI has greatly improved the resolution of the velocity model in this area and that this has subsequently improved the imaging quality. In addition to the improved seismic image, the velocity model itself provides the potential for structural interpretation; the correlation of the velocity model to the faults is striking and has led to further work to extract these features from the velocity model itself using the gradient of the velocity field in different directions. The level of detail in the FWI result also opens up the possibility of using 3D NAZ datasets for shallow geohazard detection, where the water depth is too shallow to allow 3D seismic reflection techniques to produce a high enough resolution image within the towing constraints of standard NAZ acquisition.

Conclusions

We have demonstrated the application of FWI to a 3D NAZ towed streamer dataset from the Barents Sea. In this example, we show that not only has the significant resolution in the velocity model improved the imaging, but that it contains spatially consistent features that provide additional information for interpretation.

Acknowledgements

The authors would like to thank the PL 534 partnership of BG Norge, Wintershall Norge, Statoil and Faroe Petroleum Norge for their kind permission to publish the real data example. We also acknowledge BG Group and CGGVeritas for their kind permissions to publish this work, Professor Mike Warner of Imperial College for many useful discussions on 3D FWI and Andrew Irving of CGGVeritas for assistance in the project.

References

Ratcliffe, A., Win C., Vinje V., Conroy G., Warner M., Umpleby A., Štekl I., Nangoo T., and Bertrand A., 2011, Full waveform inversion: A North Sea OBS case study: 81st Annual International meeting, SEG, Expanded Abstracts, 2384–2388.
Warner, M., Umpleby, A., Stekl, I. and Morgan, J., 2010, 3D full-wavefield tomography: imaging beneath heterogeneous overburden: 72nd EAGE Conference, Workshop WS6.

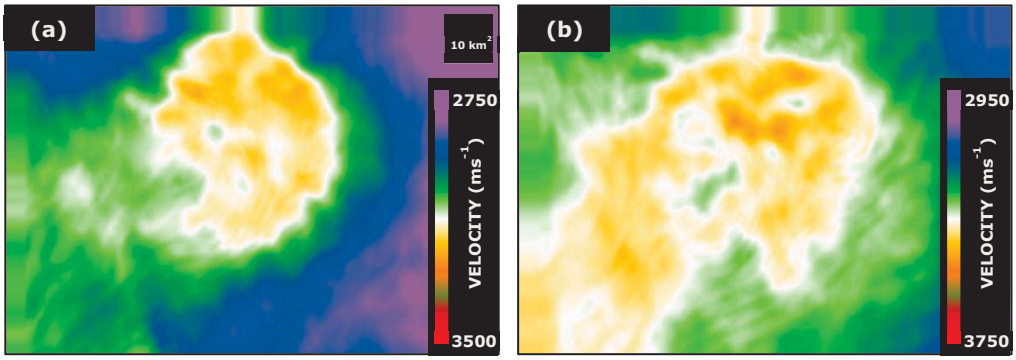

Figure 2: Depth slices through the starting velocity model at: (a) 1100 m deep, and (b) 1350 m deep.

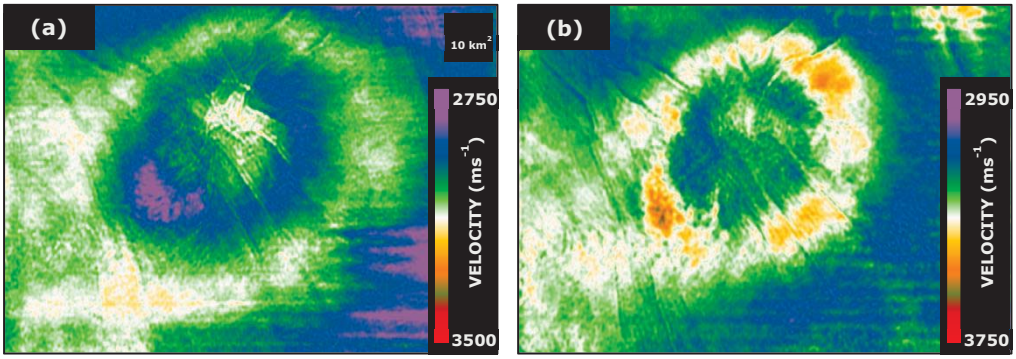

Figure 3: Depth slices through the FWI velocity model at: (a) 1100 m deep, and (b) 1350 m deep. There is a dramatic improvement in resolution of the FWI velocities compared to the starting model.

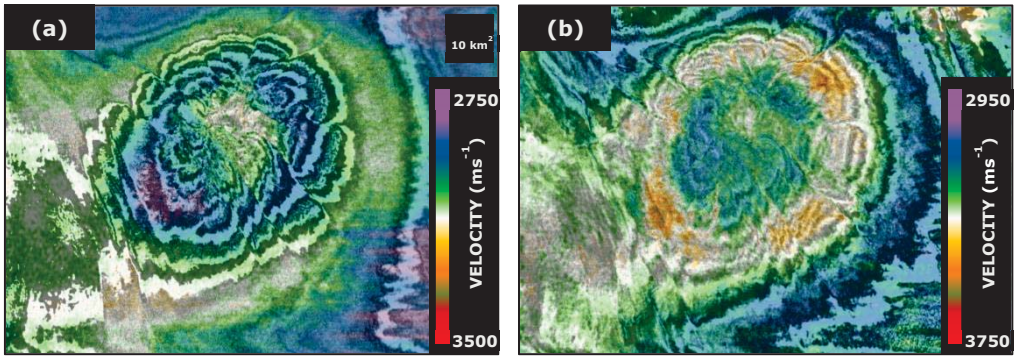

Figure 4: Depth slices through the FWI velocity model, overlaid with seismic, at: (a) 1100 m deep, and (b) 1350 m deep. Note the excellent agreement between the FWI velocity model and seismic data.

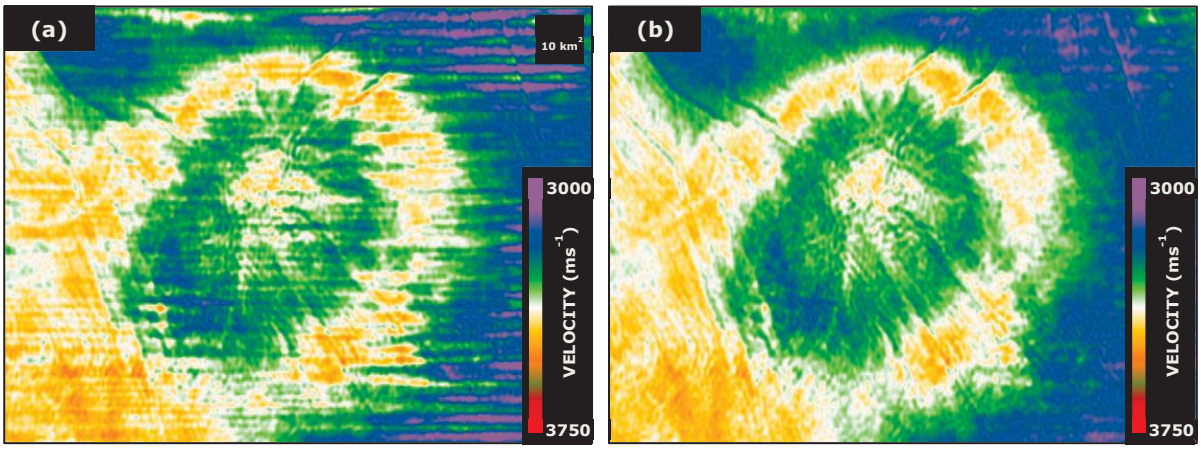

Figure 5: (a) Raw FWI model at 1420 m depth, and (b) FWI model after sail-line based footprint attenuation. Note how the resolution and detail in the velocity model has been preserved, especially in the heavily faulted regions.

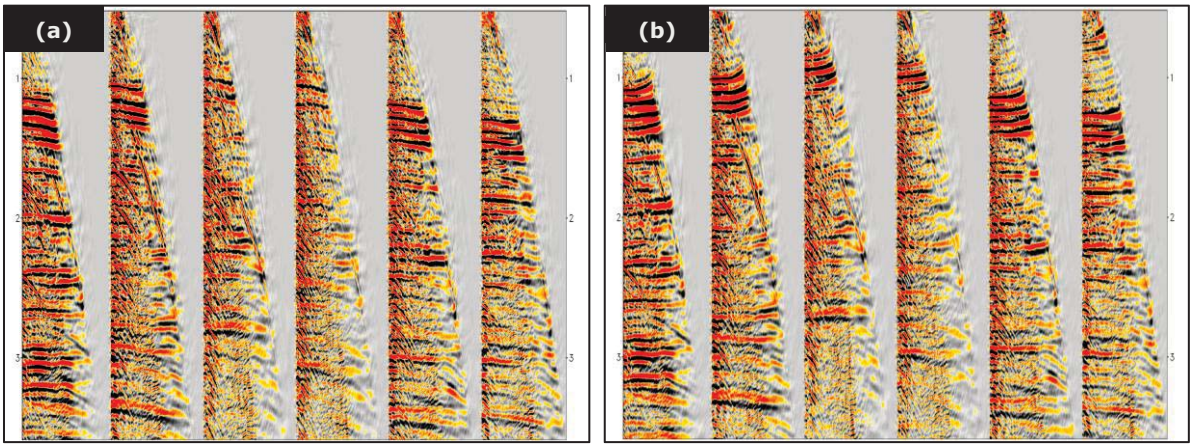

Figure 6: Common image gathers, in depth (km), generated from a migration using: (a) the starting velocity model, and (b) the FWI velocity model. The gather flatness is improved on the data migrated with the FWI velocity model.

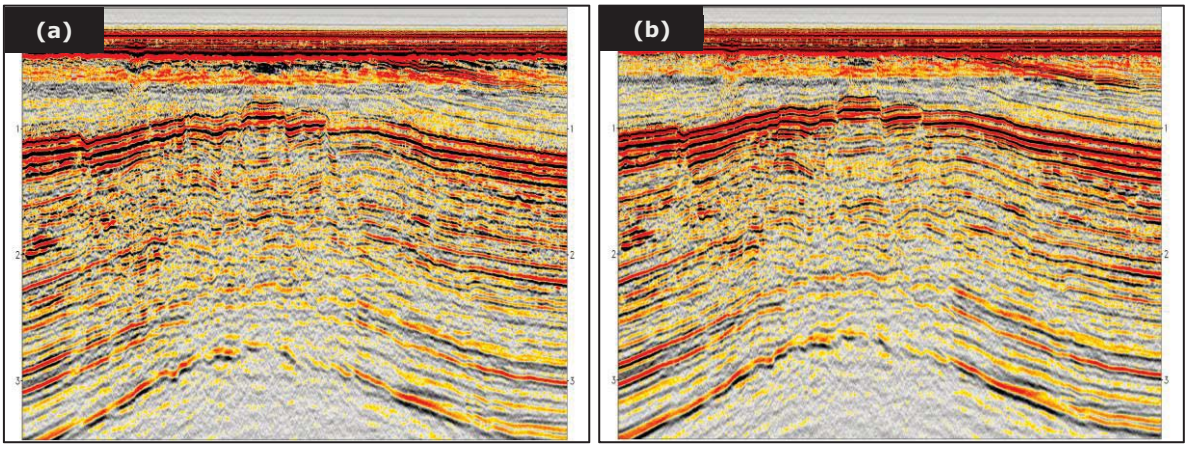

Figure 7: Migrated depth image (in km) generated from: (a) the starting velocity model, and (b) the FWI velocity model. Note the improved continuity and strength of the reflectors in the image generated with the FWI velocity model, especially in the central area.